Seismic Hazard Assessment of Syria

Raed Ali Ahmad

National Earthquake Centre, Damascus, Syria, email: raedali_2000@yahoo.com

Received: 31/07/2012
Accepted: 18/06/2013

ABSTRACT

In this paper, the well-established probabilistic seismic hazard - Poisson occurrence model - technique is applied to estimate the seismic severity of Syrian region. Syrian seismic catalog, which extends from 19 AD to 2012, as well as seismotectonic features of the region have been utilized. The seismic hazard assessment carried out using eight seismic active zones based on tectonic settings and spatial distribution of the seismic activity. We assessed the modified Gutenberg-Richter Model parameters and the maximum credible earthquake magnitude for each seismic zone. Suitable numeric attenuation models have been used for the considered seismic zones. An increment of 0.1 x 0.1 degree is used. The seismic hazard maps are developed for return periods (50, 100, 175, 475 and 975 years) and for the seven structural periods. Integrating PGA to PSA hazard maps have done based on site-effect factors of PSA/PGA. Seismic hazard curves are obtained for all major cities. Relatively high levels of PGA as well as PSA are found in regions: Lebanese part of DSFS, Al-Ghab region of Syria, along the border of Turkey and Bitilis zone. Remarkable seismicity has noticed in the eastern part of Syria.

Keywords:
Hazard maps; Response spectral acceleration (SA); Construction code; Syria; Ground motion

1. Introduction

Estimation of ground motion severity at different locations is essential for earthquake resistant design as well as for seismic safety analysis. The seismic hazard maps help in the estimation of ground acceleration (PGA or PSA) at any site. The main target of the probabilistic seismic hazard analysis is to estimate the probability that a certain PGA (PSA) will be exceeded during a known period of time at a specific site. The full representation of seismic hazard at a site is known as seismic hazard curve where PGA (PSA) is plotted against its annual exceedance probability. Although seismic hazard analysis method was developed particularly for individual sites, it can be systematically applied for a gird of points to obtain regional seismic hazard map with a certain probability level. The study area is located in the northwestern part of the Arabian plate that covers Syria, Lebanon and other neighboring countries as seen in Figure (1). Figure (1) shows the regional setting map of the northern part of the Arabian Plate and tectonic zones in Syria [1]. The main aims of the present work are: to identify seismic source models for Syria; to develop seismic hazard maps considered as the major input for anti-seismic construction code; to analyze recent recorded accelerograms extending from 1995 to 2012; to know the distributions of site-response factor at different locations in Syria (this factor show the relationships between PSA and PGA); to perform probabilistic integration of the individual influences of seismic sources into the probabilistic distribution of PGA acceleration; and finally, to generate response-spectral hazard (PSA) maps using the distributions map of site-response factor.

2. Tectonic Setting of Syria

The eastern Mediterranean and northern Arabian plates are an ideal natural laboratory for studying a

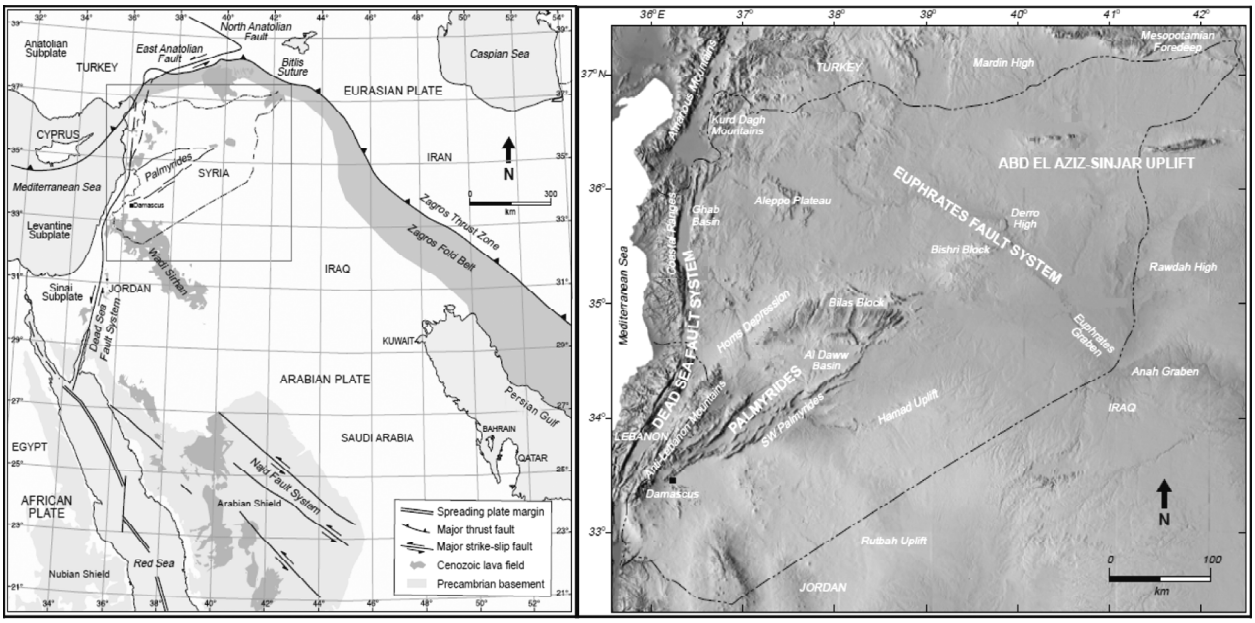

Figure 1. Regional tectonic map of Middle East Region (left), Tectonic zones in Syria (right).

variety of active tectonic processes operating in relatively small region. These processes include the Arabian-Eurasian continental collision, African subduction, and the escape of Anatolian plate [2-3]. Syria is close to the leading edge of a continent-continent collision where the Arabian Plate is converging on Eurasia at 18 ± 2 mm/year in a roughly north-northwestern direction [4]. This collision is manifest in the active transform and convergent plate boundaries, Figure (1). Deformation is focused in four major zones [5] that have been repeatedly reactivated throughout the Phanerozoic in response to movement on nearby plate boundaries. They are the Palmyride folding belt, the Euphrates Fault System, the Abd el Aziz-Sinjar uplifts, and the Dead Sea Fault System (DSFS).

3. Seismicity of Syria

There are numerous evidences of earthquake damage along the DSFS. Combining archaeo-seismology and palaeo-seismology evidences at El Hereif site show the occurrence of three large seismic events in the last 2400 years including the 1170 AD event [6]. At Saint Simeon (Qalaat Samaan), a large earthquake in 526 AD happened [7]. Historical records of Syrian region provide a rich account of damage due to the large earthquakes sequence of 1157, 1170, 1202, 1408, 1759 and 1837 [8-10]. The historical earthquakes in Syria and Lebanon reveal that a large earthquake (Ms = 7.2) occurred on July 9, 551 AD along the Lebanese littoral. Historical records of large, devastating earthquakes also provide evidence of seismic activities and seismogenic potential of the central and northern DSFS, despite the lack of moderate and large events from instrumental records. The instrumentally recorded seismological data events were collected from International Seismological Center regional catalog (ISC), U.S. Geological Survey catalog (USGS), World Data Center regional catalog (WDC), and Syrian National Earthquake Center (NEC, 2011). Historical earthquakes that occurred prior to 1900 are also collected from different sources [11-18]. Using Syrian seismicity catalog, we calculated Gutenberg's Richter parameters *a*, *b* and β as well as the magnitude of completeness mc for each zone. Various parameters of Poisson occurrence model are also obtained. The maximum curvature method (MAXC) was performed to check estimation of *mc* [19-20]. Recently, several studies show that the b value is correlated with shear stress and the variations is associated with the heterogeneity of the medium [19, 21] which influence the frequency distribution. Using Maximum Likelihood solution, we have obtained the major characteristics of Syrian catalog for the following periods of time: 19 AD to 1960, 19 AD to 1995, 1995 to 2010, 19 to 2010, 1995 to 2012 and 19 to 2012 as seen in Table (1). These parts of catalog are done to show the change of completeness magnitudes with time. These periods represent the differences in type

Table 1. The estimated Mc for time periods of Syrian catalog.

Catalog's Period	*b*	σ *b*	*a*	*a annual*	*Mc*
19 AD-1960	0.478	0.03	4.7	1.42	5
19 AD-1995	0.42	0.01	4.45	1.15	4
1995-2010	0.427	0.007	4.1	2.9	1.7
1995-2012	0.51	0.007	4.52	3.3	1.6
19 AD-2010	0.32	0.005	4.11	0.813	2
19 AD-2012	0.385	0.005	4.41	1.11	1.6

of reporting and type of recording devices. The period of 19 to 1960 represents the historical events, period of 1960 to 1995 contains events that instrumentally recorded using stations located in surrounding countries, and period of 1995 to 2012 contains the events recorded using Syrian national seismological network. The seismicity analysis is carried out based on reliable compilation of earthquake catalog obtained from different agencies. The homogeneity of the catalog is ensured, and the used historical and instrumental records are trusted. To separate the dependent from the independent seismicity, the earthquake catalog is declustered. Since mc is usually decreasing with time because the increasing number of seismic network stations and their sensitivity, the catalog has the lowest *mc* that is equal to 1.6.

4. Pobabilistic Seismic Hazard Analysis (PSHA)

Probabilistic seismic hazard analysis (PSHA) is the most widely used procedure to determine the ground motion parameters [22]. The goal of probabilistic seismic hazard analysis (PSHA) is to quantify the rate (or probability) of exceeding various ground-motion levels at a site given all possible earthquakes. Traditionally, PGA has been used to quantify ground motion in PSHA, now Response Spectral Acceleration (SA) is commonly considered since it provides the maximum acceleration experienced by a damped, single-degree-of-freedom oscillator. In references, the widely used seismic hazard maps of Syria are made for PGA as the major output such as El Hariri [23]. We could not evaluate a uniform spectral hazard using the spectral attenuation models directly since the used background of seismological data contains events that recorded at rocky-site stations (PGA) only without consideration to design accelerations (SA). Another reason is the absence of instrumental strong motion records in Syrian catalog. Thus, we had to know the relationships between PSA/PGA for each seismological station. Such ratio represents the site-response factor (S_{ki}). Analyzing recent instrumentally recorded accelerograms of small events that occurred in Syrian territory for the period of 1995 to 2012 could allow us to know the site effects for many locations in Syria. As we know, the site effects and geotechnical conditions (geological setting) under each seismic station affect the recorded accelerograms or seismograms in the same location. The value of each pixel of 0.1×0.1 degree of PGA hazard maps multiplied by site response factor (S_{ki}) that corresponded to closest seismological station k_i, and then the final hazard maps of PSA were generated. This study considers that the initial recorded peak of Accelerogram at site as PGA, while the resulted peak response spectral acceleration using SHAKE program as its PSA.

4.1. Earthquake Recurrence Models

The area source model, which realistically represents seismogenic zones, is used in the present work since the epicenters of the past earthquakes don't lie on a clear fault line, but they are scattered around many faults lines. The modified Gutenberg-Richter (MGR) - Poisson model is used due to insufficient information describing each active fault, rather performing a characteristic model in our seismic hazard calculations. In the modified Gutenberg-Richter model, the earthquake magnitude exceedance rate is given by Eq. (1) [23].

$$\lambda(M) = \lambda_0 \frac{e^{-\beta M} - e^{-\beta M_u}}{e^{-\beta M_o} - e^{-\beta M_u}}, M_o \le M \le M_u \qquad (1)$$

where λ_0 is the exceedance rate of magnitude M_o, β is a parameter equivalent to the "b-value" for the source ($\beta = b.log(10)$), and M_u is the maximum magnitude for the source. For the earthquake occurrence of Poisson process, the probability density of the earthquake magnitude is given by this equation:

$$p(M) = -\frac{d\lambda(M)}{dM} = \lambda_0 \beta \frac{e^{-\beta M}}{e^{-\beta M_o} - e^{-\beta M_u}}, M_o \le M \le M_u \qquad (2)$$

Uncertainty in the maximum magnitude is calculated based on the variable truncated Gaussian distribution, with the following probability density

function.

$$P(M_u) = \frac{1}{\sigma\sqrt{2\pi}} \frac{\exp\left[-\frac{1}{2}\left(\frac{M_u - EM}{\sigma}\right)^2\right]}{\phi\left(\frac{M_2 - EM}{\sigma}\right) - \phi\left(\frac{M_1 - EM}{\sigma}\right)} \quad (3)$$

$$M_1 \le M_u \le M_2$$

where M_u is the maximum magnitude, and M_1 is lower limit for the maximum magnitude. Frequently, M_1 is the maximum observed magnitude, M_2 is upper limit of the maximum magnitude. This value is generally fixed based on tectonic settings, *EM*: "untruncated" expected value of M_u, that is, the expected value that M_u would have if its distribution extended from $-\infty$ to ∞, σ: "untruncated" standard deviation of M_u, that is, the standard deviation that M_u will have if its distribution extended from $-\infty$ to ∞.

5. Characteristics of Seismic Sources

The seismic hazard estimates are derived from regional seismogenic zones that are based interpretations and assumptions relating potential seismic activity to the seismotectonics of the region. Based on seismicity and tectonic settings of Syria, we have considered eight seismic sources, Figure (2), Lebanese segment of DSFS (LDSF), Ghab segment of DSFS (GDSF), Bitilis zone (Southern part of Anatolian fault tectonic system) (ATF), Aleppo tectonic feature (ALP), Euphrates fault system (EPHS), Palmayride folding system (TAD), Abd-Alziz tectonic zone (ABDS), and Jabal Alarab tectonic zone (JAR). The obtained sources parameters are provided to CRISIS version 7.2 program [23-24]. Various seismic sources parameters are shown in Table (2). Using the entire Syrian seismic catalog, the magnitudes of completeness *mc*, the Gutenberg's-Richter parameters (*a*, *b*, *a*-annual), and the standard deviation of *b* have been obtained for each seismic source using maximum curvature method, see the upper part of Table (2). In calculations, the appeared parameters in the lower part of Table (2) are used. In order to perform Poisson occurrence model, we had to first define the threshold magnitude of M_0. In the current work, we have defined $M_0 = 5$ for all seismic sources, because the starting point for the design of buildings and structures begin to resist an earthquake measuring 5 on the Richter scale. Thus, all earthquakes less than $M = 5$ were removed from catalog. The new values of *b* are reflected in β (β = 2.3 x *b*) and its standard deviation αβ. The relation between area/rupture length and magnitude is: $A = K_1 e^{k_2 M}$ (for area sources, A in km^2). K_1, K_2 values are given for

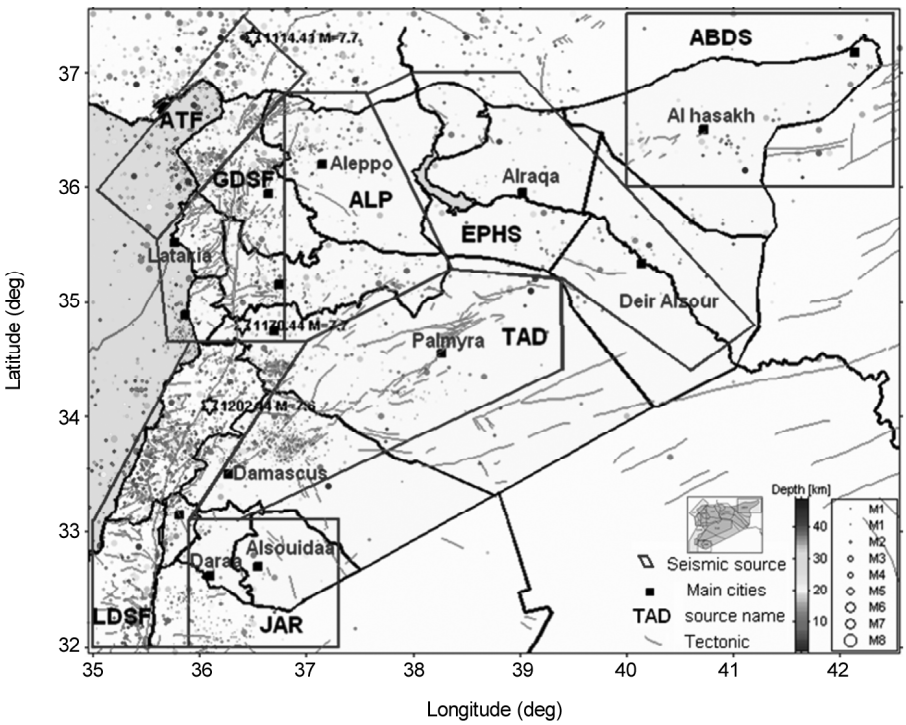

Figure 2. The proposed seismic sources in Syria.

Table 2. Seismic sources parameters used in the present study.

Using Maximum Likelihood Solution					
Zones	***b***	**σ*b***	***a***	***a annual***	***mc***
ATF	0.41	0.02	3.26	0.0318	1.8
GDSF	0.407	0.03	3.01	-0.282	1.3
LDSF	0.4	0.01	3.67	0.368	2
ALP	0.373	0.04	2.68	-0.486	1.6
TAD	0.444	0.04	3.01	-0.261	2.1
EPHS	0.404	0.06	2.51	0.6	2.4
ABDS	1.03	0.3	5.89	3.91	4.6
JAR	0.323	0.08	2.24	-0.8922	3.2

Using Weichter Algorithm (Threshold Magnitude=5)

Zones	M_0	$\lambda(M_0)$	β	σβ	Un. (M_u)	σ (M_u)	M_1	M_2	K_1	K_2
ATF	5	0.066	1.52	0.02	7.8	0.6	6.8	8	0.011	1.036
GDSF	5	0.0569	1.28	0.1	8.3	0.554	8	8.5	0.011	1.036
LDSF	5	0.12	1.68	0.07	8	0.728	7.5	8.5	0.011	1.036
ALP	5	0.0321	1.83	0.3	7	0.797	6.8	7.2	0.00564	1.1513
TAD	5	0.061	1.86	0.17	7.5	0.8	7	8	0.0101	1.048
EPHS	5	0.061	1.86	0.17	6.5	0.807	6	7	0.0101	1.048
ABDS	5	0.0707	1.98	0.12	7.5	0.86	7	8	0.0101	1.048
JAR	5	0.0144	1.44	0.3	7	0.627	6.8	7.2	0.0207	0.944

different fault type (Strike-slip, Generic, normal, Reverse). For strike-slip fault, the values of K_1 and K_2 are equal to 0.011 and 1.036 respectively. Using Gaussian distribution of earthquakes from $M_0 = 5$ to M max, three curves are produced; the Lower limit curve M_1 (minimum); Upper limit M_2 (maximum); the maximum observed curve $M_u(\alpha(M_u)$: its standard deviation). The values of exceedance rate of magnitude $\lambda(M_0=5)$ are obtained from the nonlinear relationship between occurrence rate per year against magnitudes of earthquake. Table (2) shows the values of $\lambda(M_0)$ for each seismic source. For Lebanese zone of DSFS (LDSF) the $\lambda(M_0=5)$ is 0.12.

5.1. ATF Zone (Bitilis Fault Zone)

This zone is located in the northern part of DSFS, which connected directly to southern part of Anatolian fault. Bitilis zone has a special crustal deformation figure as well as special movement that differs from Ghab segment of DSFS (GDSF). The source area is dominated by Strike-Slip faults type. The expected focal depth is approximately equal to 10 km (The focal earthquake depths assigned to seismic sources zones were collected from International Seismological Centre, Harvard CMT and Cornell focal mechanisms, and world seismological database centre). Strong earthquakes with magnitudes $M \approx 7$ occurred in 1114 and 1905.

5.2. GDSF Zone (Ghab Segment of DSFS)

This source area is dominated by Strike-Slip faults type. The expected focal depth is 10 km. The instrumentally recorded earthquake occurred in Latakia region in 1988 with magnitude $M = 4.6$. There are several events of historical strong earthquakes ($M > 7$) occurred in 65 *BC*, 859, 1114, 1157, 1822, and 1872.

5.3. LDSF Zone (Lebanese Segment of DSFS)

This source area is dominated by Strike-Slip faults type. The focal depth is considered to be 10 km. The maximum instrumentally recorded earthquake occurred in Safad area in 1927 with magnitude $M \approx 6.2$. Several strong earthquakes occurred in 1759 and 1202 with magnitudes bigger than 7. The length of LDSF segment could produce an earthquake with magnitude higher than 8.

5.4. ALP Zone (Aleppo Tectonic Feature)

This source area is dominated by generic and normal faults type, which is connected to Aleppo hill. The focal depth is considered to be 10 km. The recently known earthquake in this zone occurred in 1987 with magnitude $M \approx 4.8$, while the historical records show the occurrence of earthquakes with magnitude $M \approx 6.5$ in 1156 and 1157.

5.5. TAD Zone (Palmyride Folding System)

The source area is dominated by generic faults type. Focal depth is expected to be 29-30 km. The recent instrumentally recorded earthquakes occurred in 1994 and 1996 with magnitude (M> 5.6) in Bishri region and near Palmyra city respectively. In the past time history, several strong earthquakes had occurred in this zone especially in the southwestern part. The well-reported earthquake occurred in 1043 with magnitude M> 7.

5.6. EPHS Zone (Euphrates Fault System)

The source area is dominated by normal and generic faults type, which connected to Euphrates fault system. Focal depth is expected to be 20-25 km. Several earthquakes have occurred in this zone with magnitude less than 5.

5.7. ABDS Zone (Abd el Aziz-Sinjar uplifts)

The source area is dominated by generic and normal faults type. Focal depth is considered to be 30 km. The seismicity of this zone is connected to faults of Roudh Mountains and E-W striking Sinjar-Abd-Alziz fault. The recent recognized earthquake occurred in 1975 with magnitude $M\approx 5.2$, while the historical documents show that at least two earthquakes with magnitudes (M) bigger than 7 occurred in 1114 and 1216.

5.8. JAR Zone (Jabal Al-Arab Tectonic feature)

This seismic zone is located in the southern part of Syria. The recent instrumental records don't show that this zone is an active zone at the present time. The source area is dominated by normal fault types, which are connected to volcanic activity in this region. Focal depth is expected to be 15 km. In 1924, one earthquake with magnitude $M\approx 5.5$ had occurred, while the strongest historical earthquake occurred in 1181 with magnitude of $M\approx 6.7$. Another reported earthquake with magnitude of $Ms = 5.8$ occurred in 1152 [7].

6. Attenuation Relation

The ground motion model used in PSHA is referred to as an "attenuation relation". Given the typically large number of earthquakes and sites, attenuation relation must be simple and easy to compute. The most basic attenuation relation provides the ground motion level as a function of magnitude and distance, but many have other parameters to allow for a few different sites (e.g., rocks, soils and their thickness) with type of faults. Although several different attenuation relationships are available, they often differ significantly in terms of predicted values where data are lacking (e.g., short distances to large earthquakes) [23]. They also differ in case of amplification of PGA due to presence of sediments. Many scientists have shown various attenuation relations for numerous countries [22, 25, 26, 27, 28, 29, 30] based on peak of response spectral acceleration PSA instead of traditional peak of ground (PGA) acceleration. Since a local attenuation formula is not available, an attenuation model provided by CRISIS program was used in this work. There are many reasons did not help us to develop local attenuation models. These reasons are: absence of instrumental records of strong motion data; low to moderate seismicity in the present time; Syrian territory has not been exceeded by strong earthquake since 1759, and the recently establishment of Syrian Seismological Networks (1995). In calculations and with respect to faults type and the thickness of soil in each seismic zone, we have used corresponding attenuation models [29, 31, 32, 33]. Joyner and Boore distance [34] (closest distance to the projection of the fault plane on the Earth's surface) is used in probabilistic calculations as shown in Figure (3). There are four ways of measuring distance to the site, these ways are: 1) Focal, 2) Epicentral, 3) Joyner and Boore, 4) Closest distance to rupture area. Attenuation law plays a key role in the evaluation of ground and response spectrum accelerations. There are three major factors that should be included in any attenuation model: Characteristics of seismic source; wave propagation path to the site (construction), and the impact of geotechnical and geological conditions of this site. The general formula of used attenuation law could be shown as follows:

$$Log_{10}(PGA) = b_1(f) + b_2(f)(M-6) + b_3(f)\times (M-6)^2 + b_5 \log_{10} D + b_6(f)C \quad (4)$$

where PGA is the peak horizontal acceleration (g); M is magnitude of earthquake; $D = \sqrt{r_{jb}^2 + h^2}$; r_{jb} is Joyner-Boore distance; C is 0 for rocky site, 1 for soil, and 6 for deep soil; and b_1, b_2, …. b_6 and h are

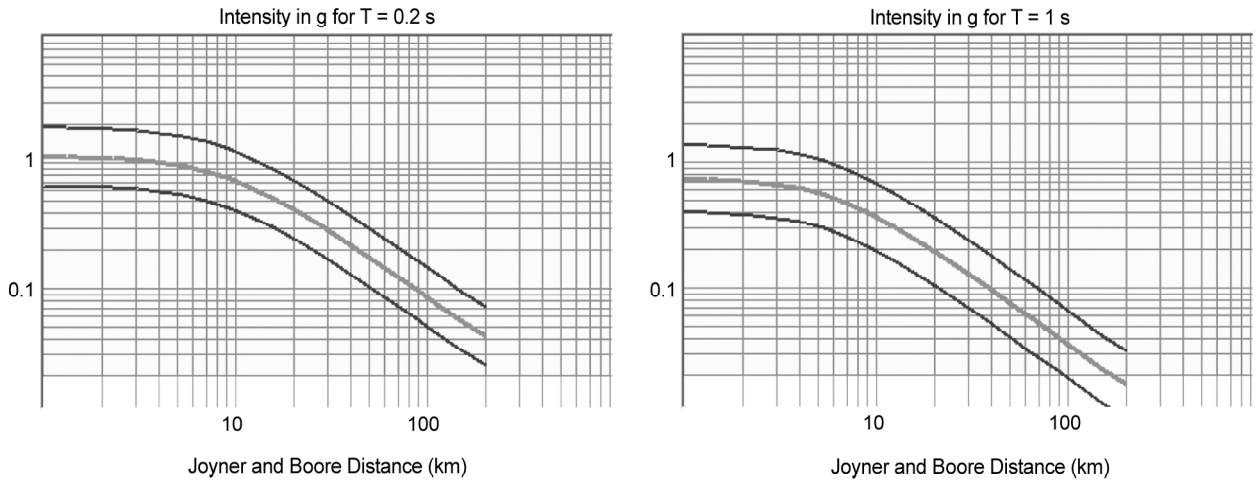

Figure 3. The Joyner and Boore distance attenuation relation used in the current work.

regression coefficients that depend on structural period. The used attenuation laws require various parameters. The parameters are: Earthquake Rupture (Magnitude, fault type); Site properties (Rock, shallow soil, deep soil, *Vs*, etc.) and Propagation effect (type of distance used, hanging wall, etc.). The parameters of each attenuation model are provided numerically to the program. These parameters are assigned for various structural periods (*T*) in seconds. In order to integrate *PGA* hazard maps to PSA hazard maps, so a number of instrumentally recorded accelerograms are collected from different locations in Syria. These accelerograms are treated by SHAKE program in order to calculate the peak response spectral accelerations (*PSA*). In order to know the site response factors distributions, the ratios of *PSA*/*PGA* (S_{ki}) are estimated. The *PGA* seismic hazard maps have been integrated to *PSA* seismic hazard maps based on the distributions of site response factors in Syria. The results show that site-response factor varies 2-4 for structural periods 0.2 to 0.3 seconds. The following formula describes the way of integrating *PGA* to *PSA* hazard map.

$$PSA_{(ij)} = PGA_{(ij)} \times S_{ki} \quad (5)$$

where *i* and *j* are the longitude and latitude of each pixel size of *PGA* and *PSA* hazard maps, and S_{ki} is the closest site factor of each seismological station (k_i).

7. Results and Discussion

In the present study, we have used the probabilistic approach of Poisson occurrence model, a number of four disaggregation distance methods: Joyner and Boore [34], epicentral, focal, and closest to rupture area, in order to perform the seismic hazard computations. Rupture radius (*R* in km) is calculated using constants of K_1 and K_2 for each fault type in each seismic source area. From earthquake catalog (19 *AD*-2012) we assessed the modified Gutenberg-Richter model parameters and the maximum credible earthquake magnitude for each seismic zone. We also used a suitable attenuation model for each seismic zone based on the dominated faults type presented; Abrahamson and Silva [31] for reverse fault type, Young et al [33] for strike-slip faults, and Garcia [29] model for normal faults. In order to get more accurate results, we have considered an increment of 0.1 x 0.1 degree for the whole area of Syria during seismic hazard computation process. Seven total numbers of spectral ordinates are used for structural period (0.005, 0.2, 0.3, 0.5, 1, 2, and 3 seconds). Here, we show the results at spectral periods 0.2 and 1.0 seconds only. We have generated seismic hazard maps in term of *PGA* first then the resulted maps have been integrated to peak response spectral maps based on the estimated ratios of site response factors of *PSA/PGA*. Figure (4) shows the seismic hazard maps for *PGA* made with respect to the following conditions: 10% probability of exceeding, 475 year return period, 50 year economic life, structural period (T = 0.2 s, up, T = 1 s, down), and (0.05, 0.01 g) contour intervals, respectively. The maximum *PGA* values founded along *DSFS* tectonic feature with *PGA* ~ 0.4-0.5 g made for 0.2 s of structural period, this value fall

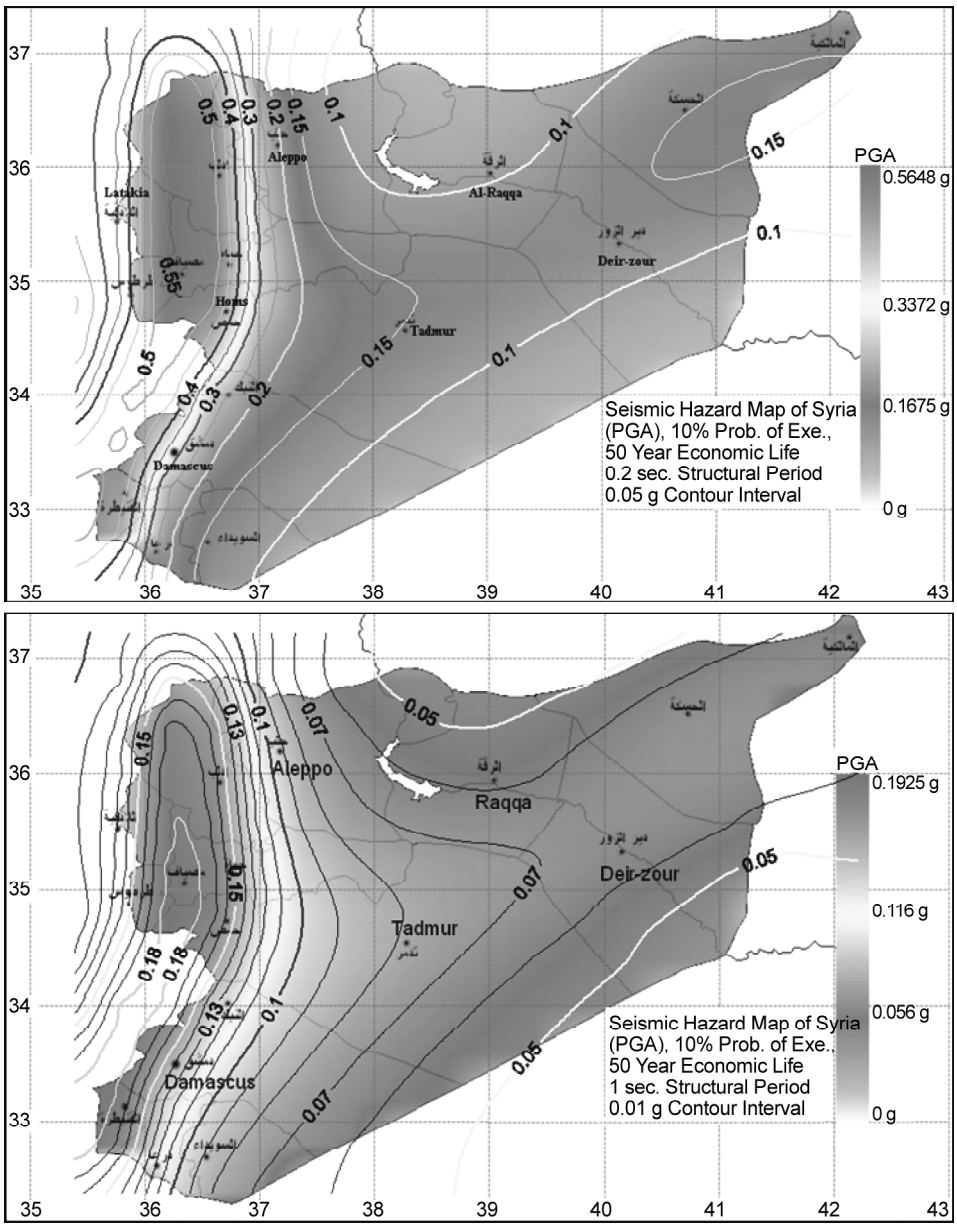

Figure 4. Seismic hazard maps of Syria for PGA acceleration, made with respect to the following conditions: 10% Probability of Exceeding, 475 Year Return Period, 50 Year Economic life, Structural Period (T=0.2s up, T=1s down), and 0.05, 0.01 contour intervals respectively.

down to reach 0.19 g for 1 second of structural period. Figure (5) shows the seismic hazard map of Syria for response spectral acceleration (*SA*) made with respect to the following conditions: 10% Probability of Exceeding, 475 Year Return Period, 50 Year Economic life, Structural Period (T=0.2 s, up, T= 1s, down), and 0.05, 0.02 contour intervals, respectively. This map shows that Bitilis fault zone has the highest value of spectral acceleration equal to 1.2 g. The spectral acceleration in the Lebanese and Syrian parts of Dead Sea Fault System (DSFS) is found to be about 1 g. The response spectral hazard map made for 1 s is found to be close to *PGA* hazard map, which is made for 0.2 s, with variations in values around 0.9 to 1.2 in comparison. The highest acceleration is located across the *DSFS* faults system. *PSA* in Lebanese part of *DSFS* and Quneitra city is equal to 0.449 g, while in the north is equal to 0.4 g. Finally, the seismic hazard maps are produced with respect to each fixed return period (50, 100, 175, 475 and 975 years). Various maps are produced for various probability of exceeding with respect to spectral periods of 0.2 and 1 sec. The return period maps for fixed ground acceleration (*PGA*) (0.1, 0.2, 0.3 and 0.4) are also estimated. The return period values of an earthquake with *PGA*=

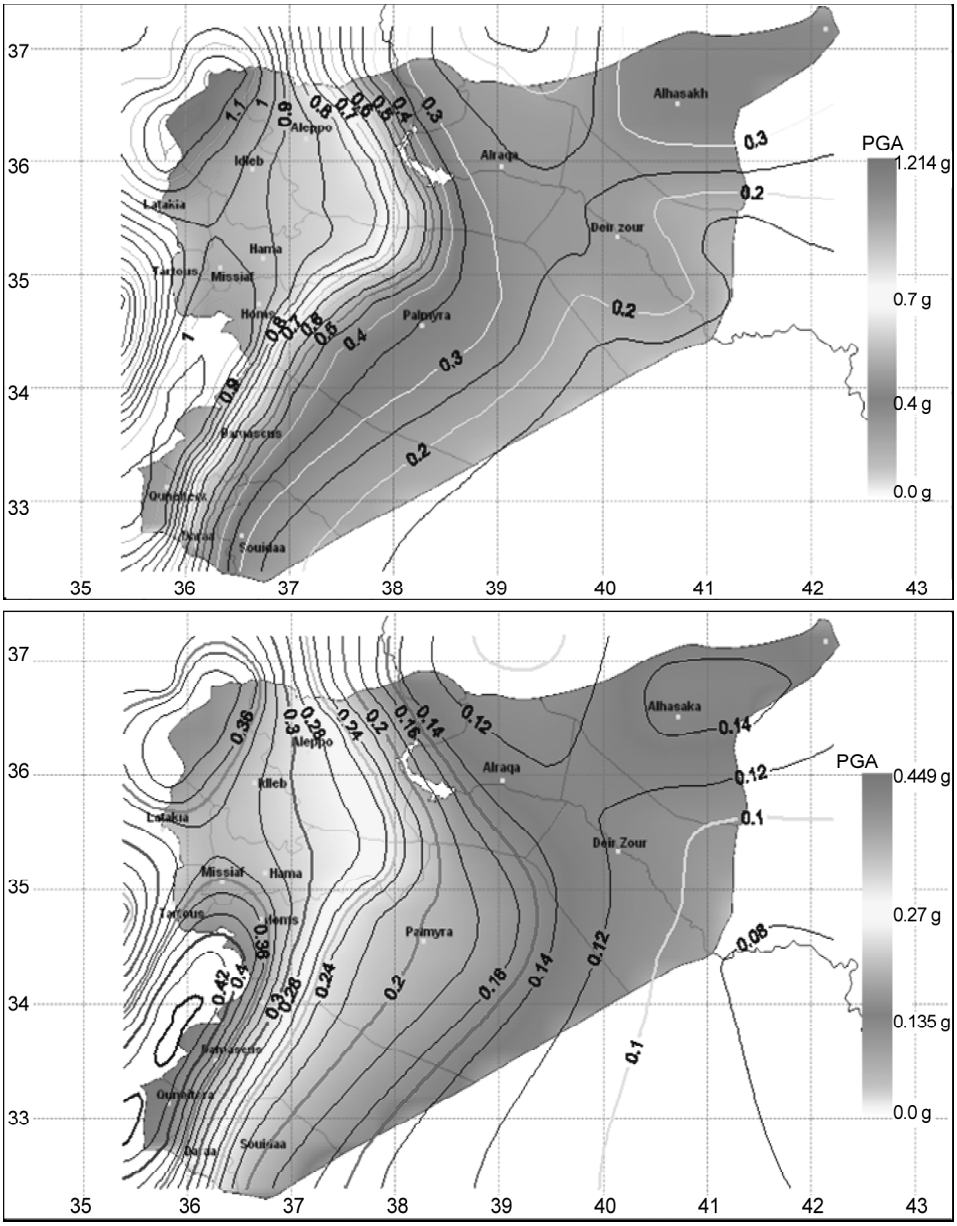

Figure 5. Seismic Hazard map of Syria for response spectral acceleration (PSA), made with respect to the following conditions: 10% probability of exceeding, 475 year return period, 50 year economic life, Structural Period (T = 0.2s up, T = 1s down), 0.05 and 0.02 contour intervals respectively.

0.2 g at 0.2 sec of structural period for Damascus city is equal to 204.4 year while it is equal to 102 year in Missiaf city, the center of Ghab section of *DSFS* fault System. Seismic hazard curves are obtained for all major cities, and these curves could be estimated for any location within Syrian territory for both types of acceleration (*PGA* and *PSA*). Figure (6) shows hazard curves for Tartous city. The linear trends appear in the bottom panels of Figure (6) are quite normal because: the return periods (earthquake recurrence time) increase with the increasing of intensity values; the relationship between return period and spectral ordinates for the same intensity take linear trends; the relationship between intensity values of *PGA* and spectral periods is inversely proportional for the same return period (this result appeared while studying response spectra of recorded accelerograms); and the expected *PGA* values are increasing with the increasing of return period. In Tartous region, Figure (6) shows that the exceeding rates of an earthquake of 0.1g are equal to 0.016 and 0.00422 at 0.2 and 1s of structural periods respectively; for 475 years of return period, the maximum acceleration is 0.38 g at 0.2 s., while the minimum acceleration is 0.15 g at 1s; the return periods of a fixed intensity of 0.1g are 62.5 and 237

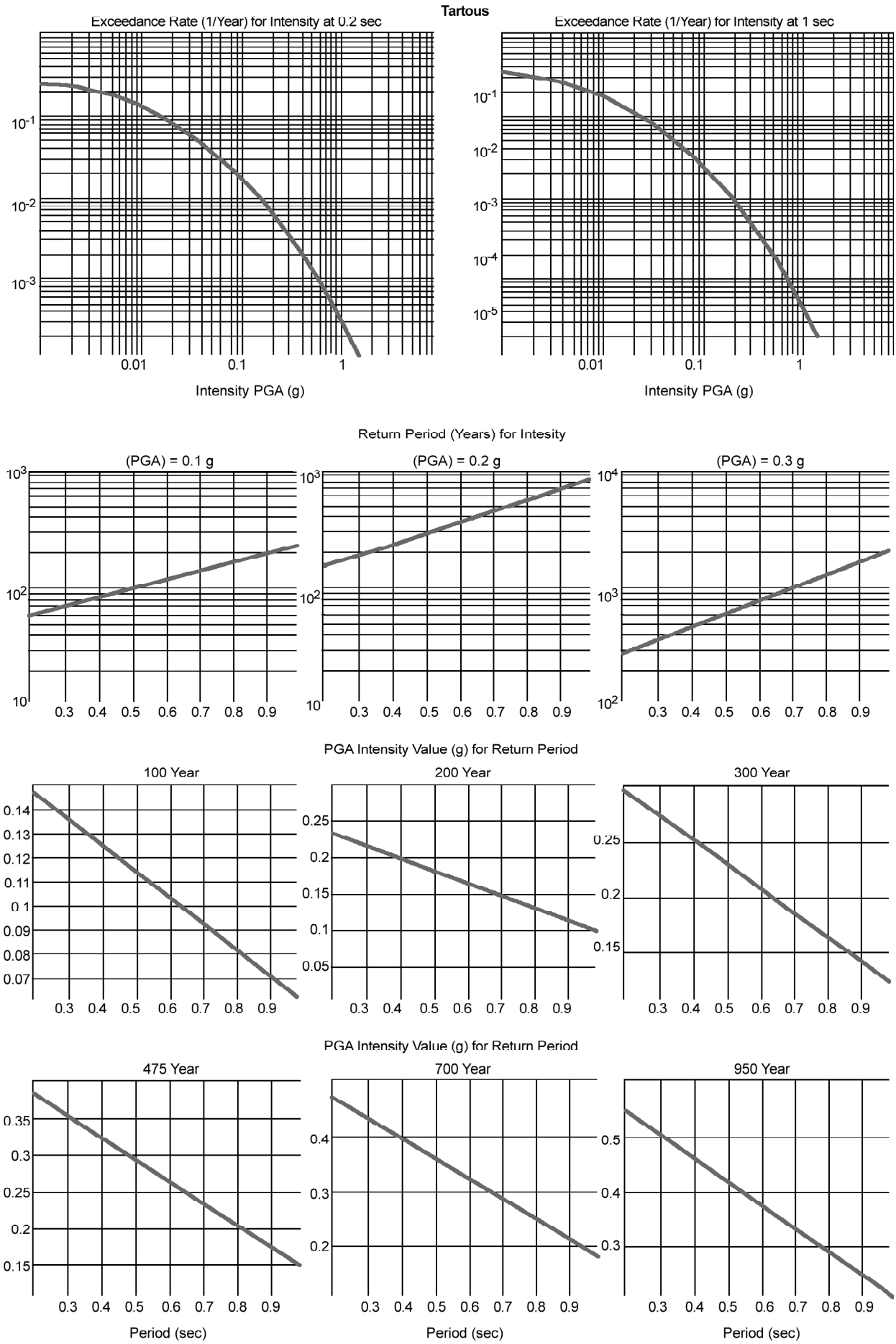

Figure 6. Estimated Seismic hazard curves for Tartous city at 0.2s and 1s of structural periods.

years at 0.2 and 1 seconds. Figure (6) presents the return periods curves for fixed intensities of 0.1, 0.2 and 0.3 g at 0.2 and 1 seconds in Tartous area. The expected ground accelerations are shown in Figure (6) for different return periods of 100, 200, 300, 475, 700, 950 years with respect to structural periods of 0.2---1s.

8. Conclusions

An analytical seismic hazard analysis is carried out for the region of Syria. Hazard curves are estimated for all major cities and several hazard maps are prepared for Syria using *PGA* and response spectral acceleration (*SA*). Return periods maps are also estimated. The present results provide a good estimate of seismic hazards and ground acceleration characteristics of Syria. These results will be of great importance to civil engineers and scientific community to design seismic codes for buildings and other various infrastructures as well as to study the spectral and ground accelerations for spectral periods of 0.2 and 1 seconds. The output hazard maps are made digitally so that one can easily estimate the desired acceleration for any location specifying coordinates (longitude and latitude). The seismic hazard map of Syria gives a good estimate of response spectral (*SA*) and *PGA* accelerations with 65, 40, 25, 10 and 5% Probabilities of Exceeding, 50, 100, 175, 475 and 975 year return periods, 50 year economic life, and varying structural periods (0.005, 0.2, 0.3, 0.5, 1, 2, and 3 seconds). The results show that Bitilis zone has the highest value of spectral acceleration equal to 1.2 g and 0.4 g, in the Lebanese part of Dead Sea Fault System (DSFS) are found to be about 1 g and 0.448 g, in the Syrian part of DSFS show close to 1 g and 0.383 g respectively at 0.2 and 1 seconds for 10% probability of exceeding and 50 years structure economic life. For return period of 975 year and 5% probability of exceeding, it is found that the spectral acceleration values vary from 1.5 g in Bitilis zone to 1.3 in Ghab segment of DSFS to 1.4 g in Lebanese part of DSFS. The maximum PGA values founded along DSFS tectonic feature with $PGA \sim 0.4\text{-}0.5g$ made for 0.2 second of structural period, this value fall down to reach 0.19 g for 1 second of structural period. The present hazard maps are based on response spectral acceleration that will be of great importance to the professional civil engineers. From the above discussions and results, the following points can be concluded:

- The level of ground and response spectral accelerations depends on the assumed probability level (degree of confidence) and the exposure period (expected economic life of the structure) and the spectral ordinates are used for structural period. The latter two parameters are related to the construction type and its importance.
- Seismic hazard maps, which include attenuation uncertainty and derived for response spectral acceleration are much more recommended for design purposes.
- The proposed hazard maps in this paper have a good agreement with seismo-tectonic features, historical seismicity, and previous hazard studies. This work also presents contour values of *PGA* and *PSA*, so one can estimate the corresponded acceleration at any given location in Syria.
- These produced maps should be included in Syrian construction code as soon as possible, and modify them when the new records of strong motion data are available.
- Even though strong motion stations (*SSA*1, *SSA*2) are available in Syria, it is recommended to develop this network and install a new strong motion network with higher number of digital strong motion sensors.
- Since the highest seismic hazard values located in the most highly populated area, obtained results from this work should be used seriously for safety requirements of existing and new structures.
- A detailed study for the attenuation characteristics of seismic waves should be carried out to provide a realistic attenuation model for each local seismic source zone with more consideration to soil site effects.

Acknowledgments

The author would like to express his gratitude to the two anonymous referees and the JSEE Editorial Board for their fruitful and valuable comments.

References

1. Brew, G., Sawaf, T., Al-Maleh, K., and Barazangi, M. (2001). Tectonic and Geologic Evaluation of Syria, *GeoArabia Gulf PetroLink Bahrain*, **6**(4), 573-615.

2. McKenzie, D. (1972). Active Tectonic of the Mediterranean Region, *Geophysical Journal of the Royal Astronomical Society*, **30**(2), 109-185.

3. Jackson, A. and McKenzie, D. (1988). The Relationship between Plate Motions and Seismic Moment Tensors, and the Rates of Active Deformation in the Mediterranean and Middle East, *Geophysical Journal*, **93**, 45-73.

4. McClusky, S. and Balassanian, S. (2000). GPS Constraints on Plate Kinematics and Dynamics in the Eastern Mediterranean and Caucasus, *Journal of Geophysical Research*, **105**, 5695-5719.

5. Barazangi, M., Seber, D., Chaimov, T., Best, J., Litak, R., Al-Saad, D., and Sawaf, T. (1993). Tectonic Evolution of the Northern Arabian Plate in western Syria, In, E. Boschi, E. Mantovani and A. Morelli (Eds.), Recent Evolution and Seismicity of the Mediterranean Region. Kluwer Academic Publishers, 117-140.

6. Guidoboni, E., Bernardini, F., Comastri, A., and Boschi, E. (2004). The Large Earthquake on 29 June 1170 (Syria, Lebanon, and Central Southern Turkey), *Journal of Geophysical Research*, **109**, B07304, doi: 10.1029/2003JB002523.

7. Sbeinati, R., Darawcheh, R., and Mouty, M. (2005). The Historical Earthquakes of Syria: An Analysis of Large and Moderate Earthquakes from 1365 B.C. to 1900 AD, *Annals of Geophysics*, **48**, 347- 435.

8. Ambraseys, N. and Melville, P. (1988). An Analysis of the Eastern Mediterranean Earthquake of 20 May 1202, in Lee, W.H.K., Meyers, H., and Shimazaki, K., eds., Historical Seismograms and Earthquakes of the World: San Diego. Academic Press, 181-200.

9. Ambraseys, N. and Jackson, A. (1998). Faulting Associated with Historical and Recent Earthquakes in the Eastern Mediterranean Region, *Geophysical Journal International*, **133**, 390-406.

10. Mouty, M. (1998). Le Jurassique du Mont Hermon (Anti-Liban). Decouverte de Trias et de Lias, Archives des Sciences et Compte Rendu, **51**(3), 295-304.

11. Syrian National Earthquake Center (NEC) (2011). Earthquakes Seismicity Data Set of Syria, Bulletins of Syrian National Earthquake Center, **1**(1-4), 1-10.

12. Alsinawi, S. and Ghalib, H.A.A. (1975). Historical Seismicity of Iraq, Bulletin of the Seismological Society of America, **65**(5), 541-547.

13. Poirier, J.P. and Taher, M.A. (1980). Historical Seismicity In the Near Middle East, North Africa, and Spain from Arabic Documents (VIIth-XVIIIth Century), Bulletin of the Seismological Society of America, **70**(6), 2185-2201.

14. Ambraseys, N. and Barazangi, M. (1989). The 1759 Earthquake in the Bekaa Valley: Implication for Earthquake Hazard Assessment in the Eastern Mediterranean Region, *Journal of Geophysical Research: Solid Earth*, **94**(B4), 4007-4013.

15. Ben-Menahem, A. (1991). Four Thousand Year of Seismicity Along The Dead Sea Rift, *Journal of Geophysical Research*, **96**(B12), 20.195-20.216.

16. Syrian Atomic Energy Organization (1992). Earthquakes or Destructive Ground Motions that Occurred In Syria and Vicinity, Seismic Intensity Map and Catalog of Historical Earthquakes in Syria. Internal Report, Syria.

17. Ambraseys, N.N. (2001). Reassessment of Earthquakes, 1900-1999, in the Eastern Mediterranean and the Middle East, *Geophysical Journal International*, **145**, 471-485.

18. Wiemer, S. and Katsumata, K. (1999). Spatial Variability of Seismicity Parameters in Aftershock zones, *Journal of Geophysical Research: Solid Earth*, **104**(B6), 135-151.

19. Wiemer, S. and Wyss, M. (2000). Minimum Magnitude of Completeness in Earthquake Catalogs: Examples from Alaska, the Western United States, and Japan.2000, Bulletin of the Seismological Society of America, **90**, 859-869.

20. Zuniga, R., Reyes, A. and Valdés, C. (2000). A General Overview of the Catalog of Recent Seismicity Compiled by the Mexican Seismological Survey, *GeoFIsica Internacional*, **39**, 161-170.

21. Menon, A., Ornthammarath, T., Corigliano, M., and Lai, G. (2010). Probabilistic Seismic Hazard Macrozonation of Tamil Nadu in Southern India, Bulletin of the Seismological Society of America **100**(3), 1320-1341.

22. El Hariri, A., (1991). Seismotectonic Study, Seismic Hazard Assessment and Zonation of the Arab Republic of Syria, M.Sc. Thesis, Institute of Earthquake Engineering and Engineering Seismology, Skopje.

23. Ordaz, M., Aguilar, M., and Arboleda, J. (2007). CRISIS2007 version 7.2: Program for Computing Seismic Hazard. Instituto de Ingenieria, UNAM, Mexico.

24. Ordaz, M. and Reyes, C. (1999). Earthquake Hazard in Mexico City: Observations Versus Computations, Bulletin of Seismological Society of America, **89**, 1379-1383.

25. Aman, A., Singh, U.K. and Singh, R.P. (1995). A New Empirical Relation for Strong Seismic Ground Motion for the Himalayan Region, *Current Science*, **69**(9), 772-776.

26. Jaiswal, K. and Sinha, R. (2007). Probabilistic Seismic-Hazard Estimation for Peninsular India, Bulletin of the Seismological Society of America, **97**(1), 318-330.

27. Singh, R.P., Aman A., and Prasad, Y.J. (1996). Attenuation Relations for Strong Ground Motion in the Himalayan Region, *Pure and Applied Geophysics*, **147**(1), 161-180.

28. Giner, J.J., Molina, S., and Jauregui, P. (2002). Advantages of Using Sensitivity Analysis in Seismic Hazard Assessment: A Case Study of Sites in Southern and Eastern Spain, Bulletin of the Seismological Society of America, **92**, 543-554.

29. Garcia, D., Singh, K., Herraiz, M., Ordaz, M., and Pacheco, J. (2005). Inslab Earthquakes of Central Mexico: Peak Ground-Motion Parameters and Response Spectra, Bulletin of the Seismological Society of America, **95**, 2272-2282, doi:10.1785/0120050072.

30. Stromeyer, D. and Grünthal, G. (2009). Attenuation Relationship of Macroseismic Intensities in Central Europe, Bulletin of the Seismological Society of America, **99**, 554 - 565.

31. Abrahamson, A. and Silva, V. (1997). Empirical Response Spectral Attenuation Relations for Shallow Crustal Earthquakes. Seismological Research Letters, **68**(1), 94-127.

32. Spudich, P., Joyner, W.B., Lindh, A.G., Boore, D.M., Margaris, B.M., and Fletcher J.B. (1999). SEA99: A Revised Ground Motion Prediction Relation for Use in Extensional Tectonic Regimes, Bulletin of the Seismological Society of America, **89**, 1156-1170.

33. Youngs, R., Chiou, J., Silva, J., and Humphrey, R. (1997). Strong Motion Attenuation Relations for Subduction Zone Earthquakes, Seismological Research Letters, **68**(1), 58-73.

34. Joyner, W.B. and Boore, D.M. (1993). Methods for Regression-Analysis of Strong-Motion Data, Bulletin of Seismological Society of America, **83**, 469-487.